Development of a 170-210 GHz 3 ×3 Micromachined SIS Imaging Array

Gert de Lange and Qing Hu
Department of Electrical Engineering and Computer Science
Research Laboratory of Electronics,
Massachusetts Institute of Technology, Cambridge, Massachusetts 02139.

Howard Huang and Arthur W. Lichtenberger
Department of Electrical Engineering
University of Virginia, Charlottesville, VA 22903

Preliminary results from a 3×3 micromachined millimeter-wave focal-plane imaging array with superconducting tunnel junctions as mixing elements are presented. The array operates in the 170-210 GHz frequency range. The micromachined array is mechanically robust and the SIS devices are sufficiently cooled. Uniform DC I-V characteristics of the different elements have been measured. We have implemented integrated tuning structures which show a 3-dB bandwidth of 70 GHz when the junction is used in a video detection mode. Preliminary noise measurements on two of the array elements resulted in lowest DSB noise temperatures of 83 K (@182 GHz) and 125 K (@184 GHz), with a bandwidth of 32 GHz and 20 GHz respectively.

1 Introduction

Imaging arrays of SIS-receivers are of great benefit for the observation of spatially extended sources in astronomy, but the high cost and mechanical difficulties of building an array of waveguide mixers and the poorer beam-quality of open-structure antennas have thus far limited the efforts of actually developing such arrays [1, 2, 3, 4, 5]. SIS-mixers made with micromachined horn antennas offer both a relatively easy, low cost fabrication and excellent Gaussian beam properties and are therefore well suited for the development of imaging arrays. Because of the specific structure of the micromachined horn antenna, interference of IF and DC-bias lines with RF antenna is avoided and also there is no limitation on the element spacing, which are problems of concern in waveguide and open structure antennas. Further advantages for the use of micromachined horn antennas in high frequency imaging arrays are the absence of substrate losses, and the possibilities of integrating a mixing element with super- or semi-conducting electronics (e.g. SQUID IF-amplifiers or Flux-Flow oscillators) [6, 7, 8]. To demonstrate the feasibility of micromachined horn antennas in imaging arrays we are currently testing a 3×3 focal plane SIS imaging array for the 170-210 GHz frequency range (the choice of the frequency range is mainly determined by the availability of the Local Oscillator and the dimensions of the cryostat). In parallel we have developed two

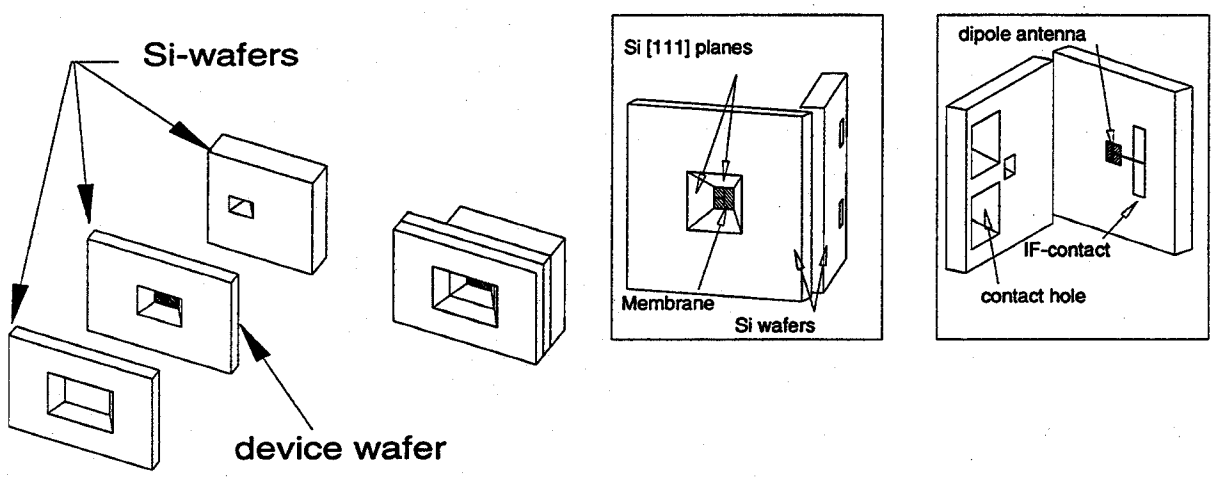

Figure 1: *(a) Overview of assembly of the micromachined horn. (b) Details of a single element of the micromachined array, showing the pyramidal cavity, the membrane, the through holes for the IF/DC connections, and the dipole antenna.*

room-temperature imaging arrays with thin-film Nb as bolometers for the 70-110 GHz and 170-210 GHz frequency range [9].

Micromachined horn antennas consist of a dipole antenna fabricated on a thin ($\sim$ 1 μm) Si_3N_4 dielectric membrane inside a pyramidal cavity etched in silicon (see Fig. 1)[10, 11]. We previously developed a single-element micromachined SIS receiver for the W-band frequency range, which showed a sensitivity comparable to the best waveguide and quasi-optical open-structure receivers [12].

This paper describes the design and fabrication of the 3×3 170-210 GHz imaging array receiver and preliminary noise measurements on the array performance.

2 Receiver Design

The array receiver can be divided into four main parts: the machined horn array, the micromachined array, the magnet, and the IF-output/DC-bias board. An expanded view of the receiver and some details of the individual elements are shown in Figs. 2, 3, and 5.

2.1 Micromachined array

The micromachined array is made of a stack of 4 Si wafers with a total thickness of 1.7 mm. The dipole antenna on the membrane is 0.58 mm long (0.37 λ). In order to have access to the contact pads on the device wafer, through holes are etched in the two wafers forming the apex of the horn (see Fig. 1). A detailed description of the individual micromachined antenna elements and the quasi-integrated horn antenna is given in [13, 14]. The stack of Si wafers forming the micromachined section is aligned with a small x-y-θ stage and the jug for holding the machined horn array. The jug and the alignment stage are positioned with respect to each other with dowel pins. To align two wafers to each other, the wafers are mounted with bee-wax to the alignment stage and to a microscope slide glued to

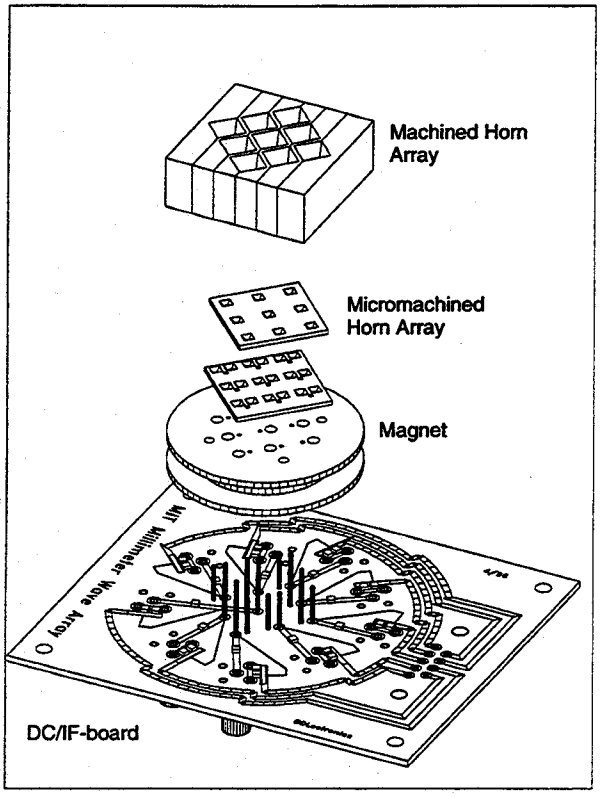

Figure 2: *Expanded view of the array receiver showing the machined horn array, the micromachined array, the magnet, and the DC/IF-board*

the jug. After alignment a small amount of superglue is used to bond the wafers together. The stage is then heated to remove the stack of wafers from the microscope slide. A similar procedure is used to align the micromachined array to the machined array. A typical accuracy of alignment is 20-40 μm.

Two serially connected $Nb/Al_2O_3/Nb$ SIS junctions are used as mixer element whose resistance is matched to the 35-Ω real impedance at the dipole antenna terminals. Typical devices fabricated at the University of Virginia facility have an area of 2.5 μm^2 and a maximum current density of 10 kA/cm^2. For our design, junctions with a current density of 5 kA/cm^2 are required. To optimize the radiation coupling to the capacitive SIS devices, two different types of on-chip tuning structures are implemented, as shown in Fig. 3a. The first type uses an inductive length of microstrip line shorted with a low impedance $\lambda/4$ stub. The low impedance stub has a 90 nm thick ($\epsilon_r = 40$) Nb_2O_5 dielectric and has dimensions of 10×35 μm^2. The microstripline is 6 μm wide and its characteristic impedance is 10 Ω for a 300 nm, ϵ_r=5.6 SiO dielectric layer . Microstrip lengths of 43 μm and 53 μm are used to accommodate variations in the fabrication process. In the second type of tuning structure a capacitive short of the coplanar feedlines of the antenna is used to form an inductive shunt similar to the tuning structure described in Ref [15]. The dimensions of the capacitive short are 20×10 μm^2 (with a 90-nm thick Nb_2O_5 dielectric) and distances of 15 and 17 μm between the junction and the edge of the capacitor are implemented.

The size of a single array element on the device wafer is much smaller than the element spacing and the vacant

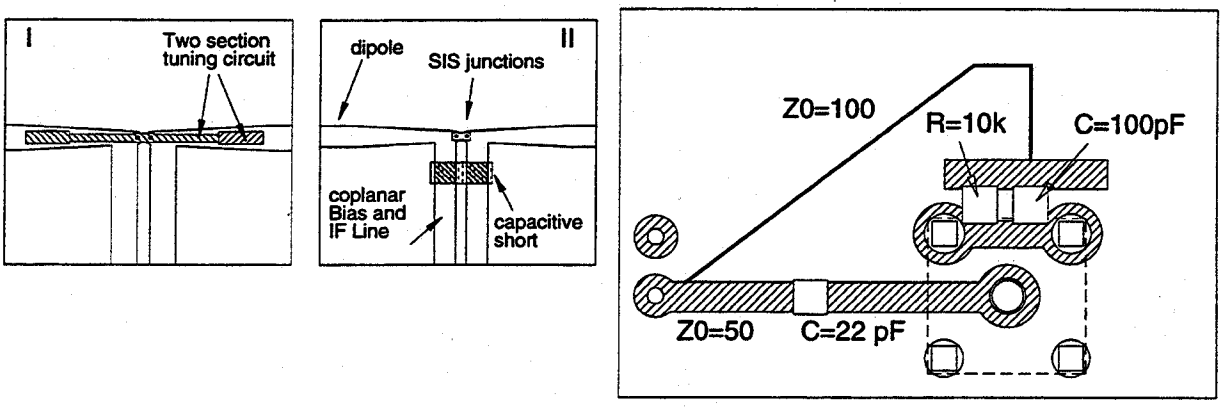

Figure 3: *(a) Details of the two different types of tuning structures incorporated in the mask design. I:two-section stub. II:capacitively shorted coplanar stub. (b) T-bias circuit.*

space on the device wafer is filled up with additional array elements to a total of 36. The positioning of the aperture and backing wafers selects the nine elements forming the array. In the current mask set, four different designs are implemented in order to find an optimum design of integrated tuning structure. In a future design identical devices will be implemented. A single fabrication run will then yield four identical 3×3 arrays.

2.2 Machined Horn Array

The geometry of the machined horn section is similar to the diagonal horn described in Ref [16]. Arrays of diagonal horns can be made with a high packing density and are relatively easy to fabricate on a milling machine with a split block technique. The array is formed by a stack of six gold plated tellurium copper blocks and fabricated at MIT Lincoln Laboratory. To assure the alignment of the separate blocks during the fabrication, a fixture is used in which the blocks are positioned by two dowel pins and mounted under a compound angle. Fabrication of machined arrays for frequencies up to a THz seems to be feasible.

2.3 Optics

As shown in Fig. 2, the minimum spacing of the individual elements of the array is determined by the aperture dimensions of the machined diagonal horn section. For the 200 GHz array the element spacing is 6.5 mm, which is $\sim$ 3.5 beam waist (the $1/e^2$ beam angle of the horn is 16°). The angular separation θ_r of the parallel beams from the array, separated by a distance d, in combination with a lens or reflector of focal length f is $\approx d/f$, whereas the 3dB beam angle θ_{3dB} of a beam with input beam waist w_{in} is 0.59 w_{in}/f. A maximum sampling of the sky requires a 3 dB beam overlap and thus $\theta_r = 2\,\theta_{3dB}$ which gives an element separation of $d = 1.18\,w_{in}$. Our array therefore undersamples the sky, as any horn array will do since the beam waist of the horn is always considerably smaller than the aperture dimensions of the horn [2].

Quasi-integrated horn antennas can be used as a feed for reflector antennas without additonal lenses. Because of the limited diameter (5 cm) of the 77 K heat filter (a 5 mm thick PTFE disk) and the dewar window (a 25 μm thick sheet of polypropylene) in the measurement set-up, a PTFE lens with a focal lenght of 37 mm is used in our set-up, to avoid truncation of the array beams. This lens is at 4.2 K. A second lens (at room temperature) with

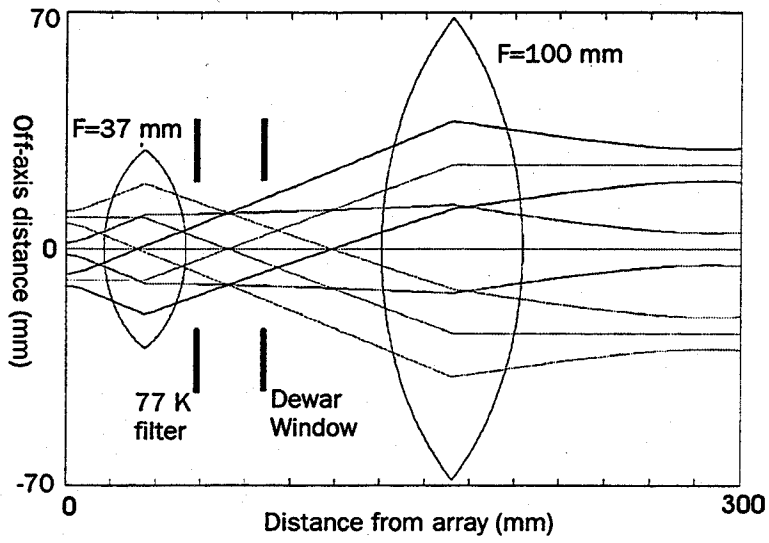

Figure 4: *Optics for the 200 GHz SIS imaging array. The figure shows the beams for the array elements on the diagonal of the array. The F=37 mm lens is located in the dewar.*

a focal length of 100 mm is used to form a gaussian telescope (See Fig. 4). The combination of the two lenses forms a slightly magnified image of the array elements at a 20-cm distance in front of the dewar. This lens set-up is convenient for our test receiver, since we can use a small hot/cold load for the heterodyne measurement and the array is reasonably uniformly illuminated if we use a beam splitter between the two lenses to couple the LO.

2.4 Magnet and DC-IF Board

A single magnet coil (made of copper) with approximately 2500 turns of superconducting 100 μm thick Nb wire (Supercon T48B) is used to suppress unwanted Josephson effects. The geometry of the micromachined array allows the magnet to be in very close proximity of the junction ($\sim$ 1.5 mm). Although the positioning of the magnet (with the magnetic field lines perpendicular to the junction surface) is not preferable, a magnet current of 200-300 mA is sufficient to suppress Josephson effects. The magnet produces a non-uniform magnetic field over the area of the array. Small permanent magnets or magnet coils located in the core of the magnet could be used to correct for this non-uniformity, but are not implemented yet.

In order to have local access to the array elements, through holes are etched in the backing wafers. This avoids the use of long coplanar lines on the device wafer (to bring the signals to the border of the wafer) and thereby increases the available space for mixer elements, reduces possible cross-talk between the different elements, and increases the flexibility of the receiver design. Contact between the array elements and the DC/IF board is made by a modified spring loaded contact pin and a short section of semi-rigid cable in which the center conductor is replaced by a spring loaded contact pin. The spring loaded contact pins are modified by cutting off the sealed end of the pin and extracting a part of the spring located inside the pin. This spring is then used as a flexible contact, instead of the original head. To ensure a reliable contact between the contact pads and the spring contact, the small cavities formed by the through holes in the backing wafers are filled with silver epoxy. The contact pin and the section of semi-rigid cable are mounted in feed through holes in the core of the magnet coil (see Fig. 5). For each array element, one contact pad is connected to the common ground (the core of the magnet) while the other contact

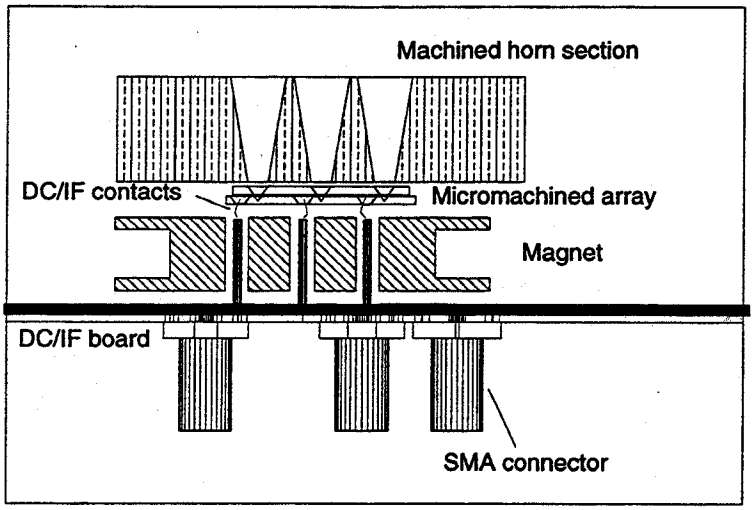

Figure 5: *Details of the receiver assembly*

pad is connected to the DC-IF board via the section of semi-rigid cable. The use of the feed through holes in the copper core of the magnet provide an effective way of shielding IF contact pins for the different elements from each other. In a previous design (without a magnet) severe cross-talk and spurious noise effects were observed in the IF-output signals

The IF/DC-board is made of Duroid 6010 material and contains a T-bias circuit for each array element. Contact between the contact pins and the microstrip line and groundplane on the IF board is made by using tight fitting sockets, soldered on the IF-board. Details of the T-bias design are shown in Fig. 3b. A 50-Ω microstrip line (width=1170 μm) (DC blocked with a 22 pF chip capacitor) connects on one end to the center conductor of a SMA connector and on the other end with the socket for the contact pin. The DC-bias is applied via a 100-Ω $\lambda/4$ line (w=152 μm, l=21 mm), capacitively shorted with a 100 pF capacitor (and a 10-kΩ resistor, to avoid charge build-up).

The array operates with a single IF-amplification stage. Noise measurements on different elements of the array are done by connecting the IF-amplifier to the different IF-ports on the DC/IF Board. The cold stage of the IF-chain consists of a Pamtech LTE 1268K isolator, and a Berkshire Technologies L-1.5-30HI IF-amplifier (40 dB). A further amplification of 60 dB is provided by room-temperature amplifiers outside the dewar. The IF-power is measured in a 35 MHz bandwidth with an HP-436A power sensor at a center frequency of 1.25 GHz (set by a tunable bandpass filter).

3 Device fabrication

The micromachined SIS arrays are made partially at MIT Lincoln Lab and partially at the University of Virginia. The SIS devices are fabricated on 0.38 mm thick (100)-oriented silicon wafers, covered on both sides with a 1-μm thick, low-stress Si_3N_4 layer. The first fabrication step is a reactive ion etch to define the apertures on the aperture side of the wafer, which will later serve as the etch mask in the anisotropic KOH-etch. The next step defines marks (with an Au lift-off) on the other (device) side of the wafer, that are references to the apertures. The patterning of

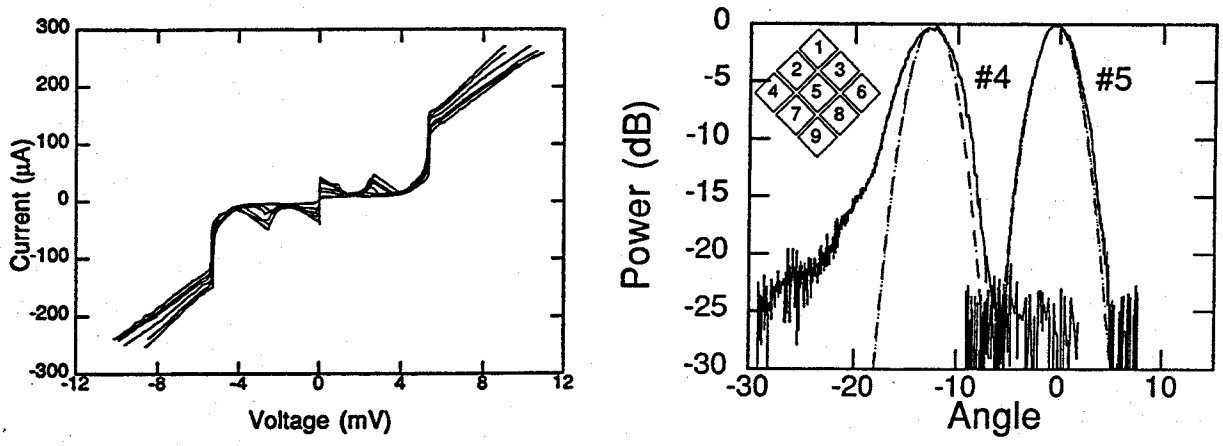

Figure 6: *(a) DC I-V curve of 7 SIS devices of the 9 element array. (b) Measured antenna beam patterns for two elements on the diagonal of the imaging array. The inset shows the device numbering.*

these marks is done using an infrared mask aligner. The marks serve as alignment marks for the antenna definition. The wafers are then shipped to UVA, where the antennas and SIS junctions are fabricated with a modified Selective Niobium Etch Process, described in [17]. Back at MIT the chip is mounted in a Teflon KOH etching mount which isolates the front and back sides of the wafer by sandwiching the wafer between two o-rings. The freestanding membrane is formed by etching the silicon in a solution which contains 20% KOH by weight at 80 ^{0}C for 4-5 hours and another hour at 60 ^{0}C. The last step is used to create smooth sidewalls of the aperture. The final fabrication step is the deposition by E-beam evaporation of a 400-nm Ti/Au layer on the sidewalls of the aperture through a ceramic shadow mask.

4 Results

4.1 DC measurements

A uniform noise performance of the different elements in an array receiver for astronomical observations is of major importance, since an increase in noise temperature of one or more of the elements rapidly reduces the advantage of using an array receiver. This is of special concern for micromachined and quasi-optical array receivers, where one defective element requires replacement of the whole device wafer.

We have thus far tested one device wafer, and results of the DC I-V measurements of 7 SIS devices in the array are shown in Fig. 6a (in this measurement the cryogenic DC contact was not optimized yet, and two devices lost contact during cool-down). The measurements are performed with the mixerblock mounted in the vacuum dewar (at a bath temperaure of 4.2 K). As shown in Fig. 6a the I-V characteristics are fairly uniform, with a $35 - 40\ \Omega$ junction resistance range. The individual elements of the array are sufficiently cooled and show no gap reduction in comparison with an I-V measurement in a LHe bath. Since the overall noise performance of an SIS receiver is not very critical to small changes in subgap current or device resistance, the device uniformity shown in Fig. 6a should be sufficient to obtain a uniform noise performance.

4.2 Antenna Pattern Measurement

As a preliminary test of the antenna patterns of the separate elements in the array, the 45-degree antenna patterns of two elements are measured at a frequency of 182 GHz. The 45-degree plane antenna are obtained by measuring the video response of the elements while rotating the dewar with a rotation stage. Due to the 45 degree angle of the array with respect to the optical table, a combined co- and cross- polarisation is measured. The two elements are at the center and outermost postion on the diagonal of the array, with the antenna beams parallel to the optical table. In this measurement, only the cold lens inside the dewar is used. The measured antenna patterns are shown in Fig. 6b, together with a Gaussian beam profile. The measured radial separation of the beams is 12.5°, and the 10 dB beamwidth of the central beam is 6.8°. Calculated values (using a thin lens approximation) for the beam separation and beam width are 14.4° and 5.2°, respectively. The off-axis element is somewhat wider and shows a non-symmetric shoulder at -17 dB, which we attribute to abberations caused by the lens. Previous measurements of single element quasi-integrated horn antennas [11] and single element [18] and arrays of diagonal horns with waveguide feeds [16] have shown excellent Gaussian antenna beam profiles at frequencies close to 1 THz. Recent measurements on our 95 GHz room-temperature bolometer also show excellent beam properties [19]. Although more thorough tests of the beam patterns of the array have to be performed, our measurements indicate the applicability of quasi-integrated horn antennas in array receivers.

4.3 FTS measurements

The frequency response of the different integrated tuning structures is measured with a Fourier Transform Spectrometer (FTS). The FTS uses a Hg-arc lamp as the broadband millimeter wave source, and is operated in the step-and-integrate mode. In these measurements the devices are biased at a voltage just below the gap voltage and used as a video detector. Fig. 8a shows the result of the measured frequency dependent coupling of three different integrated tuning structures, together with the coupling of a device without integrated tuning structure ([14]). The two section stub with a stub length of 53 μm shows a large increase in bandwidth in comparison with the device without an integrated tuning structure. The peak in the response of this device around 180 GHz is a result of the optimum coupling of the dipole antenna at this frequency. The origin of the observed peak at 300 GHz, which is also observed for the tuning structure with a 43 μm stub length, has not been identified. The tuning stucture with a capacitive short located on the coplanar feed line at 17 μm from the junctions has an optimum coupling at 130 GHz.

4.4 Noise measurements

Results of heterodyne measurements with two elements of the array with the 53-μm long two-section tuning stub are shown in Figs. 8 and 7b. The signal and LO-power are combined by a 97% transmission beam splitter and the IF-power is measured in a 35 MHz bandwidth at a center frequency of 1.25 GHz.

Fig. 8a shows the pumped DC I-V curve and IF-output power of device #4 (see the inset of Fig. 6b for the numbering of the device location) measured at a 182 GHz LO frequency. The maximum Y-factor (measured at the first photonstep below the gap voltage) is 3.7 dB, which results in a 83 $\pm$ 3 K DSB receiver noise temperature (without any correction). Analysis of the receiver noise temperature shows that the mixer gain is -1.4 $\pm$0.8 dB and the mixer noise temperature is 23 $\pm$ 8 K. The IF amplifier noise is 13.6 K (calibrated with the shot noise of the unpumped junction), which gives a total noise contribution of the IF stage of 30 K. The manufacturers specification of the amplifier noise is 4-5 K, which indicates that the current IF-coupling scheme can be substantially improved.

Fig. 8b shows the pumped DC I-V curve and IF-output power of device #7 measured at a 184 GHz LO frequency. This element has a minimum receiver noise temperature of 125 K DSB. As can be seen in Fig. 8a and b, there is a significant difference in the behaviour of the elements under irradiation with LO-power. Device #4 shows photon steps with a width of $2 \times \hbar\omega/e$, as expected in a series array of two junctions; whereas device #7 shows no

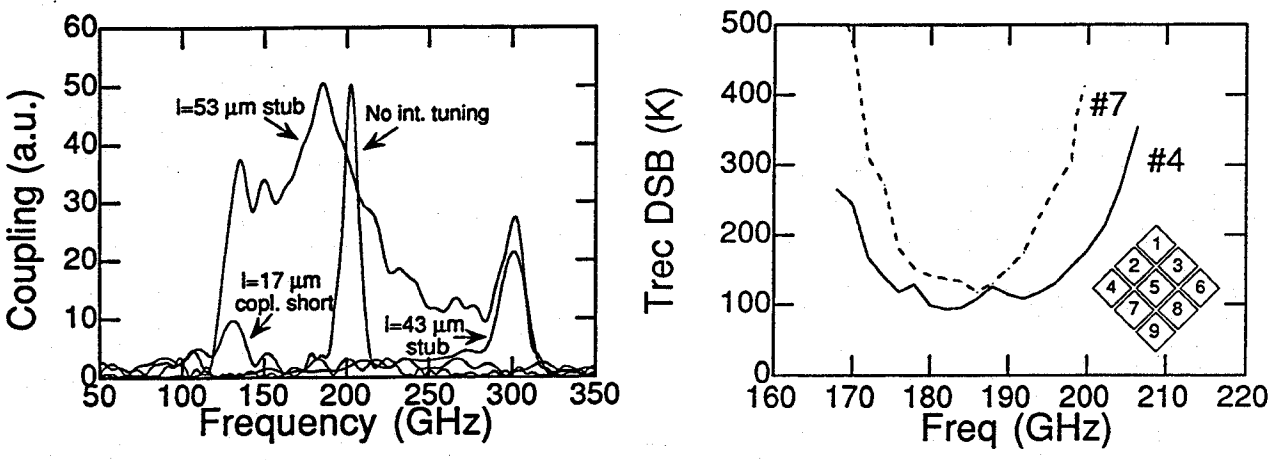

Figure 7: *(a) FTS Measurement of the three devices with different integrated tuning stucture, and one device without integrated tuning structure (b) Receiver Noise temperature for two elements of the imaging array*

clear photon steps below the gap voltage and a structure in the IF-output power of width $\hbar\omega/e$. We contribute this undesirable effect to a non-uniform division of the applied DC-bias voltage and LO-power accross the series array of junctions. At frequencies where the geometric capacitance of the junction is tuned out by the integrated tuning circuit, the junction RF-admittance is determined by the quantum susceptance. Since the quantum susceptance is a sensitive function of bias voltage (especially near the gap voltage), small differences in bias voltage between the two junctions could have a significant effect on the coupling of LO-power. Use of single junction mixers will avoid this type of non-uniformity.

The measured noise temperature as a function of frequency for these devices is shown in Fig. 7b. The 3-dB noise bandwidth for elements #4 and #7 is 32 GHz and 20 GHz respectively. We contribute the difference in the measured bandwidth to the different behaviour of the mixer elements, as explained in the previous paragraph. In a previous measurement on a single element mixer with a backing plane tuned antenna, a bandwidth of 6 GHz was measured [14], showing the effectiveness of the integrated tuning structure in the current design.

Current state-of-the-art waveguide receivers for the 230 GHz astronomy band have DSB noise temperatures of 35-50 K [19, 20, 21]. With a further optimization of the IF coupling and the use of single junction mixer elements, the fabrication of micromachined arrays with a competitive noise temperature for each array element seems feasible. Furthermore, the scalability of the machined and micromachined sections show the promising prospect for the use of micromachined focal plane imaging arrays for frequecies up to 1 THz.

5 Summary

We have described the design and fabrication of a SIS micromachined 3 × 3 focal plane imaging array for the 170-210 GHz range. Measurements show that the micromachined array can withstand thermal cycling and that the devices are sufficiently cooled. Uniform DC I-V characteristics of the different elements have been measured. The use of integrated tuning structures significantly improved the bandwidth of the mixer. Preliminary heterodyne

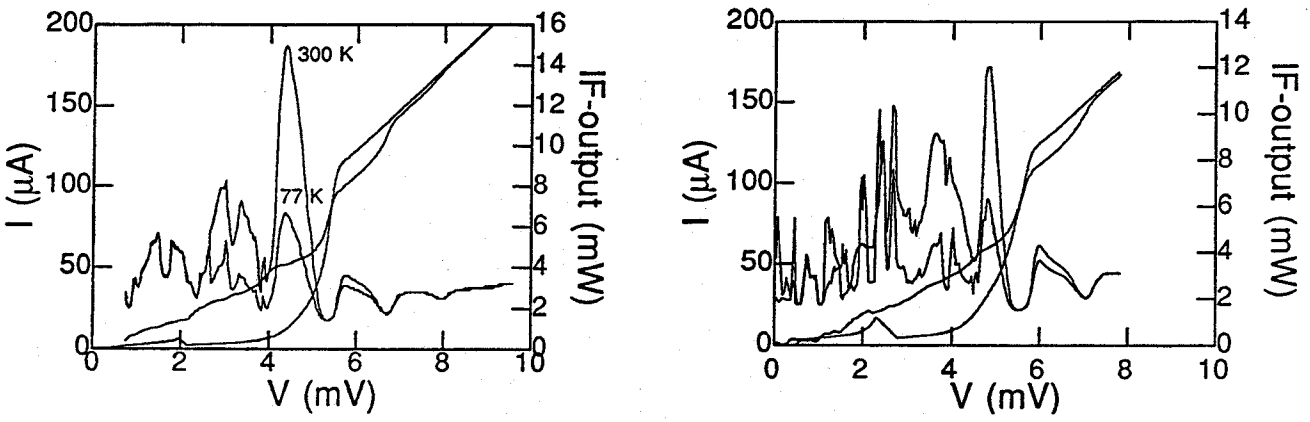

Figure 8: *(a) Pumped I-V characteristics of element #4 at a LO frequency of 182 GHz and the measured IF-output power with a 295 and 77 K input load. (b) Same measurement as in a, but for element #7 and a LO frequency of 186 GHz*

noise measurements on the array elements showed a lowest DSB noise temperature of 83 K with a 3-dB bandwidth of 32 GHz.

6 Acknowledgement

We would like to thank Earle Macedo, Dan Baker,Rich Ralston, Gerry Sollner, Rick Magliocco, Lewis Tedstone, Glenn Willman and William Cummings at MIT Lincoln Laboratory for their help during the fabrication of the devices and the fabrication of the machined horn section. Richard Bradley and Anthony Kerr are acknowledged for their useful suggestions on the dewar and IF-board design. We thank Erik Duerr, Arifuhr Rahman, and Kostas Konistis for their usefull suggestions and help during the measurements. This work was supported by the National Science Foundation under grant No. 9423608-AST, and by NASA under grant No. NAGW-4691.

References

[1] J.M. Payne, *Multibeam Receiver for millimeter-wave radio astronomy*, Rev. Sci. Instrum. **59**, 1911 (1988).

[2] Neal R. Erickson, Paul F. Goldsmith, G. Novak, Ronald M. Grosslein, P.J. Viscuso, Ronna B. Erickson, and C. Read Predmore, *A 15 element Focal Plane Array for 100 GHz.*, IEEE Trans. on MTT **40**, 1 (1992).

[3] Philip A. Stimson, Robert J. Dengler, Peter H. Siegel, and Henry G. LeDuc, in *Proc. of the Third Int. Symp. on Space Terahertz Techn.*, Univ. of Michigan (Univ. of Michigan, Ann Arbor, 1992), pp. 235–242.

[4] P.F. Goldsmith, C.-T Hsieh, G.R. Huguenin, J.Kapitzky, and E.L. Moore, *Focal Plane Imaging Systems for Millimeter Wavelengths*, IEEE Trans. MTT **41**, 1664 (1993).

[5] M.A. Scherschel, G.A. Ediss, R. Güsten, K.H. Gundlach, H. Hauschildt, C. Kasemann, A. Korn, D. Maier, and G. Schneider, in *Proceedings of the Sixth International Symposium on Space Terahertz Technology*, Caltech (Caltech, Pasadena, 1995), pp. 338–343.

[6] John A. Wright, Svetlana Tatic-Lucic, Yu-CHong Tai, William R. McGrath, B. Bumble, and H. LeDuc, in *Proceedings of the Sixth International Symposium on Space Terahertz Technology*, Caltech (Caltech, Pasadena, 1995), pp. 387–396.

[7] J.W. Kooi, M.S. Chan, M. Bin, Bruce Bumble, H.G. LeDuc, C.K. Walker, and T.G. Phillips, *The Development of an 850 GHz Waveguide Receiver Using Tuned SIS Junctions on 1 μm Si_3N_4 Membranes*, Int. J. of IR and MM waves **16**, 1 (1995).

[8] S.V. Shitov, V.P. Koshelets, A.M. Baryshev, I.L. Lapitskaya, L.V. Filippenko, Th. de Graauw, H. Scaeffer, H. van de Stadt, and W. Luinge, in *Proceedings of the Sixth International Symposium on Space Terahertz Technology*, Caltech, (Caltech, Pasadena, 1995), pp. 324–337.

[9] Arifur Rahman, Gert de Lange, and Qing Hu, *Micromachined room-temperature microbolometers for millimeter-wave detection*, Appl. Phys. Lett. **68**, 1 (1996).

[10] G.M. Rebeiz, D.P. Kasilingam, Y. Guo, P.A. Stimpson, and D.B. Rutledge, *Monolithic millimeter-wave two-dimensional horn imaging arrays.*, IEEE Trans. Antennas and Propagation **AP-38**, 1473 (1990).

[11] G.V. Eleftheriades, W.A. Ali-Ahmad, L.P. Katehi, and G.M. Rebeiz, *Millimeter-wave integrated horn antennas: Part I: Theory*, IEEE Trans. Antennas and Propagation **AP-39**, 1575 (1991).

[12] Gert de Lange, Brian R. Jacobson, and Qing Hu, *A low-noise micromachined millimeter wave heterodyne mixer with Nb superconducting tunnel junctions*, Appl. Phys. Lett. **68**, 1862 (1996).

[13] G. de Lange, B.R. Jacobson, and Qing Hu, *Micromachined millimeter-wave SIS-mixers*, IEEE Trans. Appl. Supercond. **5**, 1087 (1995).

[14] G. de Lange, B.R. Jacobson, A. Rahman, and Qing Hu, in *Proc. of the Sixth Int. Symp. on Space Terahertz Techn.*, Caltech (Caltech, Pasadena, California, 1995), pp. 372–386.

[15] S.K. Pan, A.R. Kerr, M.J. Feldman, A.W. Kleinsasser, J.W. Stasiak, R.L. Sandstrom, and W.J. Gallagher, *An 85-116 GHz SIS Receiver Using Inductively Shunted Edge Junctions*, IEEE Trans. MTT **37**, 580 (1989).

[16] Joakim F. Johansson and Nicholas D. Whyborn, *The diagonal horn as a sub-millimeter wave antenna*, IEEE Trans. MTT **40**, 795 (1992).

[17] Arthur W. Lichtenberger, Dallas M. Lea, Robert J. Mattauch, and Frances L. Lloyd, *Nb/Al-Al_2O_3/Nb Junctions with inductive tuning elements for a very low noise 205-250 GHz Heterodyne receiver*, IEEE Trans. MTT **40**, 816 (1992).

[18] H. van de Stadt, A. Baryshev, P. Dieleman, Th. de Graauw, T.M. Klapwijk, S. Kovtonyuk, G. de Lange, I. Lapitskaya, J. Mees, R.A. Panhuyzen, G. Prokopenko, and H. Schaeffer, in *Proceedings of the Sixth International Symposium on Space Terahertz Technology*, Caltech, (Caltech, Pasadena, 1995), pp. 66–77.

[19] Arifur Rahman, Erik Duerr, Gert de Lange, and Qing Hu, *Micromachined room-temperature microbolometers for millimeter-wave detection and focal plane imaging arrays*, submittted for the Proceedings of the SPIE's 11th International Symposium on Aerospace/Defense Sensing, Simulation, and Controls, Orlando, April 1997.

[20] J.W. Kooi, M. Chan, T.G. Phillips, B. Bumble, and H.G. LeDuc, *A low noise 230 GHz Heterodyne Receiver Employing .25 μm^2 Area Nb/AlO$_x$/Nb Tunnel Junctions*, IEEE Trans. MTT **40**, 812 (1992).

[21] J.W. Kooi, M. Chan, B. Bumble, H.G. LeDuc, P.L. Schaeffer, and T.G. Phillips, *180-425 GHz low-noise SIS waveguide receivers employing tuned Nb/AlOx/Nb tunnel junctions*, Int. J. IR and MM Waves **15**, 783 (1994).

[22] A.R. Kerr, S.-K. Pan, A.W. Lichtenberger, and D.M. Lea, *Progress on Tunerless SIS Mixers for the 200-300 GHz Band*, IEEE Microwave and Guided Wave Lett. **2**, 454 (1992).